Scrape-off layer modeling with kinetic or diffusion description of charge-exchange atoms

M. Z. Tokar

Citation: Phys. Plasmas **23**, 122512 (2016); doi: 10.1063/1.4972538
View online: http://dx.doi.org/10.1063/1.4972538
View Table of Contents: http://aip.scitation.org/toc/php/23/12
Published by the American Institute of Physics

Scrape-off layer modeling with kinetic or diffusion description of charge-exchange atoms

M. Z. Tokar
Forschungszentrum Jülich GmbH, Institut für Energie- und Klimaforschung - Plasmaphysik, Partner of the Trilateral Euregio Cluster (TEC), 52425 Jülich, Germany

(Received 31 August 2016; accepted 2 December 2016; published online 22 December 2016)

Hydrogen isotope atoms, generated by charge-exchange (c-x) of neutral particles recycling from the first wall of a fusion reactor, are described either kinetically or in a diffusion approximation. In a one-dimensional (1-D) geometry, kinetic calculations are accelerated enormously by applying an approximate pass method for the assessment of integrals in the velocity space. This permits to perform an exhaustive comparison of calculations done with both approaches. The diffusion approximation is deduced directly from the velocity distribution function of c-x atoms in the limit of charge-exchanges with ions occurring much more frequently than ionization by electrons. The profiles across the flux surfaces of the plasma parameters averaged along the main part of the scrape-off layer (SOL), beyond the X-point and divertor regions, are calculated from the one-dimensional equations where parallel flows of charged particles and energy towards the divertor are taken into account as additional loss terms. It is demonstrated that the heat losses can be firmly estimated from the SOL averaged parameters only; for the particle loss the conditions in the divertor are of importance and the sensitivity of the results to the so-called "divertor impact factor" is investigated. The coupled 1-D models for neutral and charged species, with c-x atoms described either kinetically or in the diffusion approximation, are applied to assess the SOL conditions in a fusion reactor, with the input parameters from the European DEMO project. It is shown that the diffusion approximation provides practically the same profiles across the flux surfaces for the plasma density, electron, and ion temperatures, as those obtained with the kinetic description for c-x atoms. The main difference between the two approaches is observed in the characteristics of these species themselves. In particular, their energy flux onto the wall is underestimated in calculations with the diffusion approximation by 20%–30%. This discrepancy can be significantly reduced if after the convergence of coupled plasma-neutral calculations, the final computation for c-x atoms is done kinetically. *Published by AIP Publishing.* [http://dx.doi.org/10.1063/1.4972538]

I. INTRODUCTION

By recombination of charged plasma components on the divertor target plates, limiters and vessel wall of fusion devices neutral particle species are generated. These recycle back into the plasma volume and participate in diverse interactions with electrons and ions, essentially affecting the plasma state.[1] By charge-exchange collisions with ions, the so-called c-x atoms of a broad velocity spectrum are produced so that a kinetic description of these particles seems to be mandatory. Such a description is performed usually by statistical Monte Carlo methods,[2] whose main problem is the high level of accident errors, "noise." This leads normally to a significant deterioration in the convergence of the plasma model coupled to the neutral module, and self-consistent neutral-plasma simulations turn into an extremely time consuming numerical procedure. For example, the calculations of two-dimensional plasma profiles in the scrape-off layer (SOL) and divertor, done in the framework of the ITER project,[3] required a central processing unit (CPU) time of months on the modern computers. Therefore, it is very attractive to use the reduced hydrodynamic approximations for neutrals which can be realized without "noise." Recently,[4] it has been proven, by describing the c-x atoms in a detached divertor, that the diffusion approximation, being formulated for the atom pressure, provides results very close to those obtained by integrating the kinetic equation. It is, however, not surprising for the conditions of very low temperatures of plasma components considered in Ref. 4. Indeed, in such a case, the rate coefficient for atom ionization by electrons, k_{ion}, is much smaller than that of their charge-exchange with ions, k_{cx}. Therefore, during the life time of an atom till ionization it undergoes a lot of charge-exchange collisions, leading to chaotic changes in the atom velocity, so that its motion is like diffusion.

Out of the divertor, in the main part of the SOL, the dominant source of neutral species is the plasma recycling on the first wall of the machine vessel. The temperatures of electrons and ions vary across the SOL very steeply, by approaching the level of hundreds of electron-volts near the separatrix. Under such conditions, a diffusion approximation for c-x atoms is not rigorously valid since k_{ion} is comparable with k_{cx}, and the characteristic scales for the plasma parameter variation in the radial direction—to the penetration depth of atoms. Therefore it is of a significant interest to assess the errors which are done, by applying approximate but fast diffusion models for neutrals in the SOL region. By keeping this aim in mind and in order to perform a broad parameter study, we apply in the present work a modeling approach

"lighter" than the normally used. Presently, the 2-D kinetic Monte Carlo description for neutral particles and fluid transport equations for transfer of charged particles and heat in the plasma are normally applied to model axisymmetric tokamak devices, see, e.g., Ref. 5. Our approach relies on the averaging of original transport equations for the plasma components along the main SOL fraction. This procedure is substantiated by the results of 2-D calculations themselves, see, e.g., Ref. 6, showing the plasma parameter profiles rather flat along the flux surfaces in the SOL main fraction, out of the compact region near the X-point and divertor. Therefore they can be well represented by the values averaged along the main SOL. The variation of the averaged parameters across flux surfaces are governed by one-dimensional equations, deduced from the original 2-D ones, with the parallel particle and heat flows towards the divertor involved as additional loss terms. The kinetic modeling for c-x atoms is done by applying an iterative procedure elaborated in Ref. 7 to solve the equation for their velocity distribution function. Being formulated in the integral form,[7] this equation reveals clearly the origin of enormous CPU time spent on modeling of c-x atoms: double integrals over the normal and velocity spaces have to be calculated for every grid point at each iteration. It is demonstrated here that for the Maxwellian velocity distribution function of plasma ions, the integration over the velocity space can be done with a very high accuracy by an approximate pass method.[8] This allows to reduce the CPU time at least by a factor of 30–50, compared to direct numerical computations of the integrals, and permits to perform an exhaustive comparison of the coupled neutral-plasma calculations done with either kinetic or diffusion descriptions of c-x atoms. However, also under such an extreme speeding up of computations, the modeling of c-x atoms remains the most time demanding part. Moreover, the relevancy of this procedure in 2-D and 3-D geometries is not demonstrated yet. This makes even more important the validation of the diffusion approximation, which allows reducing the CPU time by orders of magnitude further and can be easily generalized on multi-dimensional situations.

The remainder of the paper is outlined as follows. In Section II the set of equations used to model the neutral species generated by the plasma recycling at the vessel wall is formulated. The pass method to calculate integrals over the velocity space, being involved in the kinetic equation in the integral form and the reduction in the limit $k_{ion} \ll k_{cx}$ of the kinetic description to the diffusion one, formulated for the c-x atom pressure, are also demonstrated here. The averaging of plasma transport equations along the flux surfaces in the SOL main fraction and the assessment of the loss terms due to particle and heat flows towards the divertor are performed in Section III. In Section IV computations are done for the input parameters from the European DEMO project[9,10] and the results obtained with either kinetic or diffusion description of c-x neutrals are compared. It is demonstrated that practically for all characteristics of interest, the diffusion approximation is sufficiently satisfactory. Conclusions are drawn in Section V.

II. MODEL FOR NEUTRAL SPECIES

A. Species included for consideration

The span of neutral species of hydrogen isotopes released from the first wall into the SOL plasma is defined by the phenomena at the wall surface. Electrons and ions leave the plasma due to transport processes and recombine into atoms on the wall. With the probability R^i_{bs}, being a function of the ion energy E_i, and the mass and charge of the wall particles, these atoms escape back into the plasma, with an energy $E^i_{bs} \lesssim E_i$. The rest fraction, $1 - R^i_{bs}$, of atoms give up their energy to the wall particles and recombine into molecules. Finally, the molecules of hydrogen isotopes can be released from the wall with the probability ω_{rec}. A similar situation takes place for atoms generated in the plasma by charge-exchange collisions and escaping onto the wall; R^{cx}_{bs} and E^{cx}_{bs} denote the back-scattering probability and the energy of these species. The atom species above vanish in the plasma because of the ionization and charge-exchange collisions with electrons and ions. These are characterized, respectively, with the rate coefficients k^a_{ion}, being a function of the electron temperature, and k^a_{cx}, weakly depending on the ion temperature and atom energy.[11] The decay of the densities of the back-scattered atom species, n^i_{bs} and n^{cx}_{bs}, correspondingly, with the distance x from the wall is described by the relations

$$n^i_{bs}(x) = \frac{\Gamma_p R^i_{bs}}{V^i_{bs}} \exp\left[-\frac{\int_0^x \nu^i_{bs} dx}{V^i_{bs}}\right], \tag{1}$$

$$n^{cx}_{bs}(x) = \frac{|j_{cx}(0)| R^{cx}_{bs}}{V^{cx}_{bs}} \exp\left(-\frac{\int_0^x \nu^{cx}_{bs} dx}{V^{cx}_{bs}}\right], \tag{2}$$

where Γ_p is the density of the charged particle outflow from the plasma onto the wall, $j_{cx}(x)$ the flux density of c-x atoms; $V^{i,cx}_{bs} \approx \sqrt{E^{i,cx}_{bs}/m}$ are the velocities of the back-scattered atom components with m being the atom mass; $\nu^{i,cx}_{bs} = (k^a_{ion} + k^{bs-i,cx}_{cx})n$ are the total frequencies of the atom species destruction, with the subscripts $(bs-i)$ and $(bs-cx)$ meaning k^a_{cx} calculated for the energy of the corresponding atom species, see the Appendix; n is the plasma density assumed the same for electrons and ions.

Neutral molecules released into the plasma are disintegrated in processes of dissociation and ionization by electrons and charge-exchange with ions, characterized by the rate coefficients k^m_{dis}, k^m_{ion} and k^m_{cx}, respectively. For the molecule density n_m one has

$$n_m(x) = \frac{j_m(0)}{V_m} \exp\left[-\frac{\int_0^x n\left(k^m_{dis} + k^m_{ion} + k^m_{cx}\right) dx}{V_m}\right], \tag{3}$$

where $j_m(0)$ is the molecule influx density and V_m is their mean velocity. In collisions of molecules with the plasma particles, Franck-Condon (f-c) atoms, with a characteristic energy $E_{fc} \simeq 3.5$ eV, are generated. The velocity of f-c atoms is chaotically directed, and one can introduce separately the

densities of particles moving from and towards the wall, n_{fc}^{+} and n_{fc}^{-}, respectively. The change of $n_{fc}^{\pm}$ with x is governed by continuity equations

$$\pm V_{fc}\partial_x n_{fc}^{\pm} = n\left(k_{dis}^{m} + \frac{k_{ion}^{m}+k_{cx}^{m}}{2}\right)n_m - \nu_{fc}n_{fc}^{\pm},$$

where $\nu_{fc} = n(k_{ion}^{a} + k_{cx}^{fc})$, $V_{fc} \approx \sqrt{E_{fc}/m}$ is the characteristic velocity of f-c atoms. The difference of these equations for n_{fc}^{+} and n_{fc}^{-}, respectively, provides

$$\frac{V_{fc}}{\nu_{fc}}\partial_x n_{fc} = n_{fc}^{-} - n_{fc}^{+},$$

where $n_{fc} = n_{fc}^{+} + n_{fc}^{-}$ is the total density of f-c atoms. By differentiating the latter relation once more and substituting into the sum of equations above for n_{fc}^{+} and n_{fc}^{-}, one gets a "diffusion" equation for n_{fc}

$$\partial_x\left(-\frac{V_{fc}^2}{\nu_{fc}}\partial_x n_{fc}\right) = n\left(2k_{dis}^{m} + k_{ion}^{m} + k_{cx}^{m}\right)n_m - \nu_{fc}n_{fc}. \quad (4)$$

The boundary condition for this equation at $x=0$ follows from the back-scattering condition at the wall, $n_{fc}^{+} = R_{bs}^{fc}n_{fc}^{-}$,

$$\frac{V_{fc}}{\nu_{fc}}\partial_x n_{fc} = \frac{1-R_{bs}^{fc}}{1+R_{bs}^{fc}}n_{fc},$$

and $\partial_x n_{fc} = 0$ at the plasma axis, $x = r_w$, where r_w is the wall minor radius, i.e., the distance from the plasma axis to the wall.

The distribution function of atoms generated by charge-exchange collisions with ions, φ_{cx}, is a function of x, the x-component of the atom velocity, V_x, and the kinetic energy $E_\perp$ of the atom motion in the plane perpendicular to x. The integration of the kinetic equation for c-x atoms with respect to $E_\perp$ results in the following 1-D equation for the distribution function $f_{cx}(x,V_x) = \int \varphi_{cx}(x,V_x,E_\perp)dE_\perp$,[7]

$$V_x\partial_x f_{cx} = S_{cx}\frac{\exp\left(-V_x^2/V_{th}^2\right)}{\sqrt{\pi}V_{th}} - \nu_{cx}f_{cx}, \quad (5)$$

where $\nu_{cx} = n(k_{ion}^{a} + k_{cx}^{cx})$, S_{cx} is the density of the total source for c-x atoms

$$S_{cx} = S_{cx0} + nk_{cx}^{cx}n_{cx}, \quad (6)$$

with

$$S_{cx0} = n\left(k_{cx}^{m}n_m + k_{cx}^{bs-i}n_{bs}^{i} + k_{cx}^{bs-cx}n_{bs}^{cx} + k_{cx}^{fc}n_{fc}\right), \quad (7)$$

being the source part due to charge-exchange of primary neutrals, i.e., molecules, f-c atoms and species back-scattered from the wall

$$n_{cx}(x) = \int_{-\infty}^{\infty} f_{cx}(x,V_x)dV_x,$$

is the density of c-x atoms. The adequacy of the Maxwellian velocity distribution for the charge-exchange source term in Eq. (5), with the ion thermal velocity $V_{th} = \sqrt{2T_i/m}$, has been discussed in Ref. 7. Arguments, supporting this approximation, are given also in the Appendix of the present paper.

By considering separately the c-x atoms with $V_x \lessgtr 0$, one can find the integral relations for the corresponding parts of the velocity distribution function

$$f_{cx}(x,V_x>0) = \int_0^x \frac{S_{cx}}{\sqrt{\pi}V_{th}V_x}\exp\left(-\frac{V_x^2}{V_{th}^2} - \frac{U_x-U_y}{V_x}\right)dy, \quad (8)$$

and

$$f_{cx}(x,V_x<0) = -\int_x^{\infty} \frac{S_{cx}}{\sqrt{\pi}V_{th}V_x}\exp\left(-\frac{V_x^2}{V_{th}^2} + \frac{U_y-U_x}{V_x}\right)dy, \quad (9)$$

where

$$U_{x,y} = \int_0^{x,y} \nu_{cx}dz. \quad (10)$$

By integrating f_{cx} with respect to V_x, one gets an integral equation for n_{cx},

$$n_{cx}(x) = \int_0^{r_w} \frac{S_{cx}}{\sqrt{\pi}V_{th}}I_1(\alpha_{xy})dy, \quad (11)$$

where the integral

$$I_k(\alpha_{xy}) = \int_0^{\infty} f_k(u)du, \quad (12)$$

with $f_k(u) = \frac{\exp\left(-u^2-\alpha_{xy}/u\right)}{u^k}$ and $\alpha_{xy} = |U_x - U_y|/V_{th}(y)$. By taking into account the balance of hydrogen particles in the wall, one can find the density of the molecule influx

$$j_m(0) = \omega_{rec}\frac{\left(1-R_{bs}^{i}\right)\Gamma_p + \left(1-R_{bs}^{fc}\right)|j_{fc}(0)| + (1-R_{bs}^{cx})|j_{cx}(0)|}{2},$$

where the outflows of f-c and c-x atoms are given by the relations

$$j_{fc}(0) = -\frac{V_{fc}^2}{\nu_{fc}}\frac{dn_{fc}}{dx}(0);$$
$$j_{cx}(0) \equiv \int_{-\infty}^{\infty} f_{cx}(0,V_x)V_x dV_x = -\int_0^{\infty}\frac{S_{cx}}{\sqrt{\pi}}I_0(\alpha_{0y})dy. \quad (13)$$

B. Assessment of kinetic integrals

An inspection of Equations (10)–(12) allows to see the origin of large CPU time expenditures on kinetic calculations for c-x atoms: for each grid point x, one has to calculate the enclosed double integrals over the ion velocity space and over the whole plasma volume, $0 \le y \le r_w$, and repeat this in an iterative procedure with respect to the whole profiles of $n_{cx}(x)$ and the plasma parameters. However, by looking at the shape of the function under the integral displayed in

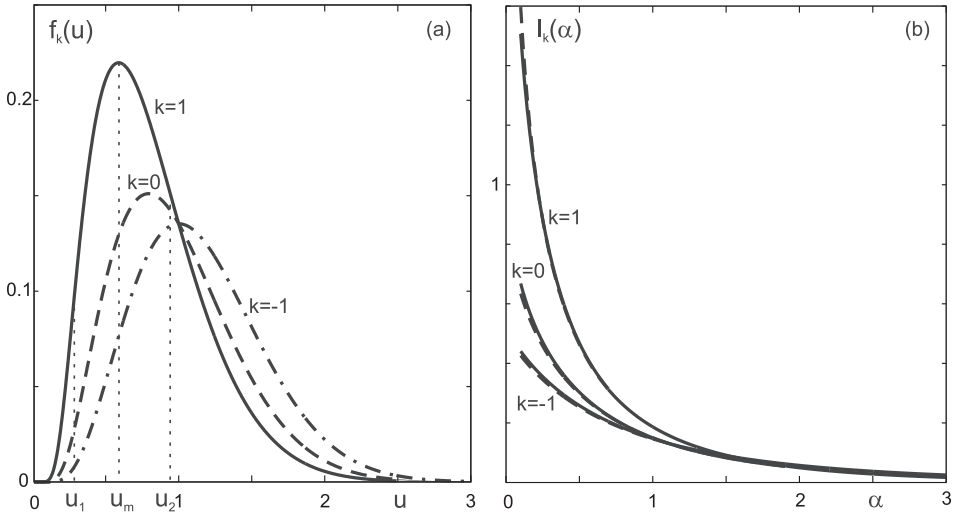

FIG. 1. The functions $f_k(u) = \exp(-u^2 - \alpha/u)u^{-k}$ for $\alpha = 1$ and $k = 1, 0, -1$; the points u_m and $u_{1,2}$ defined by the conditions $f_k'(u_m) = 0$ and $f_k''(u_{1,2}) = 0$, correspondingly (here for $k = 1$) (a); the "kinetic" integrals $I_k(\alpha) = \int_0^\infty f_k(u)du$ estimated by the pass method (solid curves) and computed numerically (dashed curves) (b).

Figure 1(a) together with functions $f_{0,-1}(u)$ for $\alpha_{xy} = 1$, one can notice: in the case under consideration, the usage of an approximate pass method[8] can be sufficiently precise and bring large time savings compared to direct numerical calculations of I_k. For each of the functions $f_k(u)$, one can distinguish 4u-intervals where it behaves principally differently: $u \le u_1$, $u_1 < u \le u_m$, $u_m < u \le u_2$, and $u_2 < u$, see Figure 1(a) where the points $u_{1,2}$ and u_m are marked for $k = 1$. These points are defined by the conditions $f_k'(u_m) = 0$ and $f_k''(u_{1,2}) = 0$, where the derivatives $f_k' = -f_k g_1/u^2$, $f_k'' = f_k g_2/u^4$ with

$$g_1(u) = 2u^3 + ku - \alpha,$$
$$g_2(u) = (g_1 + u)^2 - (1 + k + 6u^2)u^2.$$

For $k = 0$, we get $u_m = (\alpha/2)^{1/3}$; for $k = 1$ and $k = -1$ u_m is a root of a cubic equation. In the former case, this equation has a single real root $u_m = \sqrt[3]{b + a} - \sqrt[3]{b - a}$ with $a = \alpha/4$ and $b = \sqrt{a^2 + 1/216}$. In the latter one the expression for u_m above is applicable but with $b = \sqrt{a^2 - 1/216}$ and for $a \ge \sqrt{2/27}$ only. A more complex analytical expression exists also for $a < \sqrt{2/27}$. However, it is simpler and faster to use the Newton method[12] to find an approximate solution for $g_1 = 0$. By taking as the initial approximation $u_m = 1/\sqrt{2} + (\alpha/2)^{1/3}$, it requires maximally 4 iterations $u_m \to u_m - g_1(u_m)/g_1'(u_m)$ to find u_m with a relative accuracy 10^{-4} for any α. By searching for $u_{1,2}$, one can see that for the roots of interest, the equation $g_2(u_{1,2}) = 0$ reduces to the following ones:

$$h_1(u_1) = g_1(u_1) + u_1 + u_1\sqrt{1 + k + 6u_1^2} = 0,$$

$$h_2(u_2) = g_1(u_2) + u_2 - u_2\sqrt{1 + k + 6u_2^2} = 0.$$

By selecting properly the initial approximations to $u_{1,2}$, these equations are solved with the Newton method, providing accurate enough solutions after 3–5 iterations.

To assess the integrals I_k, we approximate the functions $f_k(u)$ as a linear one at $u \le u_1$ and by polynomials of the fifth order at the intervals $u_1 < u \le u_m$ and $u_m < u \le u_2$ with the coefficients selected to reproduce $f_k(u_{m,1,2})$, $f_k'(u_{1,2})$, $f_k''(u_m)$, and $f_k'(u_m) = f_k''(u_{1,2}) = 0$; in addition $f_k(u) \approx \exp(-u^2 - \alpha/u_2)u^{-k}$ is assumed for $u_2 < u$ where $\alpha/u \ll u^2$. This results in

$$I_k(\alpha) \approx \frac{f_k^2(u_1)}{2f_k'(u_1)} + \frac{f_k(u_1)\delta_1 + f_k(u_m)(u_2 - u_1) + f_k(u_2)\delta_2}{2} + \frac{f_k'(u_1)\delta_1^2 - f_k'(u_2)\delta_2^2}{10} + f_k''(u_m)\frac{\delta_1^3 + \delta_2^3}{120} + \exp\left(-\frac{\alpha}{u_2}\right)\frac{s_k}{2}, \quad (14)$$

where $\delta_1 = u_m - u_1$, $\delta_2 = u_2 - u_m$, $s_1 = E_1(u_2^2)$, $s_0 = \sqrt{\pi}[1 - \mathrm{Erf}(u_2)]$, and $s_{-1} = \exp(-u_2^2)$, with $E_1(\xi) = \int_\xi^\infty \frac{\exp(-x)}{x}dx$ being the exponential integral function. Figure 1(b) shows $I_{1,0,-1}$ versus α found with the pass method outlined above and evaluated numerically. By approximating the direct numerical results very accurately, the procedure above allows to reduce the CPU time by a factor of 30–50 at least.

As an alternative to the usage of formula (14), one can calculate in advance the integrals $I_k(\alpha)$ as functions of α and save this in a table. Then, by solving Equation (11) for any particular α, the integral $I_k(\alpha)$ can be interpolated from the values in the table for arguments larger and smaller than that in question. However, the searching of the correct α-interval in this table requires also some time. In the case of the most important I_1, this time grows up with $\alpha \to 0$ since $I_1(\alpha) \to \infty$ as $E_1(\alpha)$ and the density of data in the table has to be increasing. Thus, it is not obvious that the usage of tables is more time saving than the formula (14).

C. Diffusion approximation

With the usage of the pass method for the assessment of the integrals I_k, one-dimensional kinetic calculations for neutrals stand alone require 6–7 iterations to get a solution with an accuracy higher than 1%. It requires less than 3 s of the CPU time on a 1 GHz processor compared to 2 min needed for the same problem, being solved either by calculating the kinetic integrals numerically or with a Monte Carlo approach.[13] For the accuracy 10^{-6} adopted in the present study, kinetic neutral calculations require roughly 60 iterations. A converged solution of the coupled neutral-plasma

problem needs a reasonable CPU time of 30 min. Nonetheless, it is unclear whether it is possible to utilize a similar procedure in a 2- or 3-D geometry. Normally in such a case, a diffusion approximation is used for c-x atoms to avoid a huge noise. To derive this, the velocity distribution function of the particles in question is assumed as a shifted Maxwellian one and the fluid like equations are deduced for the continuity of particle density and momentum. Henceforth, by neglecting the mass velocity contribution to the inertia term, a diffusion like relation for the flux can be obtained, see, e.g., Refs. 4, 14, and 15. However, the validity of the assumptions and steps described above are not strictly proved. Therefore, we deduce here the particle flux density in a diffusion approximation directly from the velocity distribution function for c-x atoms given by the relations (8) and (9). By taking into account that x and U_x are uniquely related to each other, we introduce the variable

$$G(U_x, V_x) = \frac{S_{cx0}/n + k_{cx}^{cx} n_{cx}}{(k_{ion}^a + k_{cx}^{cx}) V_{th}} \exp\left(-\frac{V_x^2}{V_{th}^2}\right).$$

As per definition, a diffusion approximation is applicable if the mean free path length (mfpl) of particles in question is much smaller than the characteristic dimensions for the change of the parameters involved. The typical mfpl for c-x atoms is $\lambda_{cx} = V_{th}/(k_{cx}^{cx} n)$, but their total penetration depth is defined by k_{ion}^a. Thus, the diffusion approximation is relevant if $k_{ion}^a \ll k_{cx}^{cx}$. Moreover, it is required (i) $|V_x| \ll U_{x,y}$ for typical V_x, x, y and (ii) and the Taylor's expansion $G(U_y) \approx G(U_x) + \frac{\partial G}{\partial U_x}(U_x)(U_y - U_x)$ is applicable. By substituting the expansion above into the relations (8) and (9), one can easily perform the integration over U_y. By neglecting exponentially small terms proportional to $\exp(-U_x/|V_x|)$, we get

$$f_{cx}(x, V_x) \approx \frac{G(U_x, V_x)}{\sqrt{\pi}} - \frac{V_x}{\sqrt{\pi}} \frac{\partial G}{\partial U_x}(U_x, V_x).$$

Because G is an even function of V_x, the former term in $f_{cx}(x, V_x)$ does not contribute to the flux density of c-x atoms

$$j_{cx}(x) = \int_{-\infty}^{\infty} f_{cx}(x, V_x) V_x dV_x,$$

and we obtain

$$j_{cx}(x) \approx -\frac{1}{m_i k_{cx}^{cx} n} \partial_x \left(n_{cx} T_i + \frac{S_{cx0} T_i}{n k_{cx}^{cx}}\right). \tag{15}$$

By integrating the kinetic equation (5) with respect to V_x, we get $S_{cx0} + n k_{cx}^{cx} n_{cx} - n(k_{ion}^a + k_{cx}^{cx}) n_{cx}$ on the right hand side. Thus the term $n k_{cx}^{cx} n_{cx}$ is cancelled out, and one has a continuity equation for c-x species as follows:

$$\partial_x j_{cx} = S_{cx0} - k_{ion}^a n n_{cx}.$$

In the diffusion limit, the c-x atom mfpl λ_{cx} has to be much smaller than the characteristics change scale, in particular, for S_{cx0}. Therefore the contribution from the second term in j_{cx}, being of $\lambda_{cx}^2 \partial_x^2 S_{cx0}$, can be neglected compared to the term S_{cx0} on the right hand side. Thus, we get the following diffusion equation for the density of c-x atoms

$$\partial_x \left[-\frac{\partial_x (n_{cx} T_i)}{m_i k_{cx}^{cx} n}\right] \approx S_{cx0} - k_{ion}^a n n_{cx}. \tag{16}$$

The boundary condition to Equation (16) at the wall implies that c-x atoms leave the plasma with the thermal velocity, i.e., $j_{cx}(0) = -n_{cx}\sigma\sqrt{T_i/m}$ at $x = 0$, with the factor $\sigma \approx 1.07$ seems to be the best choice; $j_{cx} = 0$ at the plasma axis, $x = r_w$.

III. CHARGED PLASMA COMPONENTS

A. Basic transport equations

In the SOL, the charged plasma components, electrons, and fuel ions, are described by two-dimensional fluid equations. These govern the variations of the plasma density n, electron and ion temperatures T_e and T_i, correspondingly, across the flux surfaces, the coordinate x, and along the magnetic field, the direction l,

$$\partial_x \Gamma_\perp + \partial_l \Gamma_{||} = S_{ion}, \tag{17}$$

$$\partial_x q_\perp^e + \partial_l q_{||}^e = -E_{ion}^m S_{ion}^m - E_{ion}^a S_{ion}^a - Q_{ei}, \tag{18}$$

$$\partial_x q_\perp^i + \partial_l q_{||}^i = Q_{ai} - 1.5 S_{cx} T_i + Q_{ei}, \tag{19}$$

where $\Gamma_{\perp,||}$ are components of the particle flux density along the x and l directions, $q_\perp^{e,i} = -\kappa_\perp^{e,i} \partial_x T_{e,i} + 1.5\Gamma_\perp T_{e,i}$ and $q_{||}^{e,i} = -\kappa_{||}^{e,i} \partial_l T_{e,i} + 2.5\Gamma_{||} T_{e,i}$ the components of the heat flux densities, with $\kappa_{\perp,||}^{e,i}$ being the components of the heat conduction; $S_{ion} = S_{ion}^m + S_{ion}^a$ with $S_{ion}^m = k_{ion}^m n n_m$ and $S_{ion}^a = k_{ion}^a n (n_{bs}^i + n_{bs}^{cx} + n_{fc} + n_{cx})$, the contributions to the plasma particle source density due to ionization of molecules and atoms, respectively; E_{ion}^m and E_{ion}^a the energy spent by electrons in ionization collisions; $Q_{ai} = \nu_{bs}^i E_{bs}^i n_{bs}^i + \nu_{bs}^{cx} E_{bs}^{cx} n_{bs}^{cx} + \nu_{fc} E_{fc} n_{fc} + \nu_{cx} W_{cx}$ is energy transported to the ions by ionization and charge-exchange of atoms, with

$$W_{cx}(x) = \frac{m}{2} \int_0^\infty \frac{S_{cx} V_{th}}{\sqrt{\pi}} \left[I_1(\alpha_{xy}) + I_{-1}(\alpha_{xy})\right] dy,$$

being the heat capacity density of c-x atom; the last terms on the right hand sides of the heat balance equations, Q_{ei}, are due to the heat exchange between electrons and ions through coulomb collisions.

The boundary conditions to Equations (17)–(19) at the wall, $x = 0 (r = r_w)$, are fixed e-folding lengths of the parameters in question, $\delta_n = \partial x/\partial \ln n$, $\delta_{e,i} = \partial x/\partial \ln T_{e,i}$; at the separatrix, $x = x_s (r = r_s)$, we prescribe the plasma density $n(r_s)$ and the densities of the heat outflows from the confined plasma region, $q_\perp^{e,i}(r_s)$. Some fraction of neutrals, recycling from the wall, may penetrate through the SOL region into the confined plasma, $0 \le r \le r_s$. To take these into account, the density and temperature profiles have to be postulated there. We distinguish the edge transport barrier, $r_b = r_s - \Delta_b \le r \le r_s$, where

$$n = \varepsilon_s n(r_s) + \varepsilon_b n(r_b), \quad T_{e,i} = \varepsilon_s T_{e,i}(r_s) + \varepsilon_b T_{e,i}(r_b),$$

with $\varepsilon_s = (r - r_b)/\Delta_b$, $\varepsilon_b = 1 - \varepsilon_s$, and the core, $0 \le r \le r_b$, where

$$n = n(0)\exp(-\lambda_n r^2/r_b^2), \quad T_{e,i} = T_{e,i}(0)\exp(-\lambda_{e,i} r^2/r_b^2),$$

with $\lambda_n = \ln[n(0)/n(r_b)]$ and $\lambda_{e,i} = \ln[T_{e,i}(0)/T_{e,i}(r_b)]$. The parameters r_b, r_s, $n(0)$, $n(r_b)$, $n(r_s)$, $T_{e,i}(0)$, $T_{e,i}(r_b)$ are prescribed according to the European DEMO project,[9,10] $T_{e,i}(r_s)$ are got by solving the transport equations in the SOL.

B. Equations for parameters averaged along the SOL

As it was already stated above, we consider here the main part of the SOL, henceforth the main SOL, out of the divertor and the X-point vicinity where a significantly enhanced interaction between the plasma and neutrals often takes place. A good estimate for the extent of the main SOL along the magnetic field is two connection lengths L between the high and low field sides of the torus. To obtain equations, describing the variation in the x-direction of the parameters averaged along the main SOL, we integrate Equations (17)–(19) with respect to l in the range $0 \le l \le L$, with $l = 0$ corresponding to the symmetry plane where $\Gamma_{||}$, $q_{||}^{e,i} = 0$. As a result one gets

$$d\langle\Gamma_\perp\rangle/dx = \langle S_{ion}\rangle - \Gamma_{||L}/L, \tag{20}$$

$$d\langle q_\perp^e\rangle/dx = -E_{ion}^m\langle S_{ion}^m\rangle - E_{ion}^a\langle S_{ion}^a\rangle - \langle Q_{ei}\rangle - q_{||L}^e/L, \tag{21}$$

$$d\langle q_\perp^i\rangle/dx = \langle Q_{ai}\rangle - 1.5\langle S_{cx}T_i\rangle + \langle Q_{ei}\rangle - q_{||L}^i/L, \tag{22}$$

where $\langle\cdots\rangle = \int_0^L \cdots dl/L$, $\Gamma_{||L}$ and $q_{||L}^{e,i}$ are the densities of the parallel losses of charged particles and their energy at the end of the main SOL.

To relate $\Gamma_{||L}$ and $q_{||L}^{e,i}$ to the SOL averaged parameters, $\langle n\rangle$ and $\langle T_{e,i}\rangle$, we apply an approximate method from Ref. 16 for solving the parabolic partial differential equations, e.g., a diffusion one. This method is based on the concept that equations in question allow neither the periodic sign-changing solutions nor a similar behavior of individual terms in them. It presumes that the solution profile in a certain direction is mostly controlled by the corresponding transport term and is not very sensitive to the spatial variation of other terms. By following this presumption, we rewrite Equations (17)–(19) as follows:

$$\partial_l\Gamma_{||} = S, \quad \partial_l q_{||}^{e,i} = W_{e,i},$$

with some unknown source/sink terms S and $W_{e,i}$. By assuming these independent of l and integrating equations above from $l = 0$, we get

$$\Gamma_{||}(l)/\Gamma_{||L} = q_{||}^{e,i}(l)/q_{||L}^{e,i} = l/L. \tag{23}$$

With the relations for $q_{||}^{e,i}$ above and by adopting the Spitzer-Härm approximation for the parallel heat conduction,[17] $\kappa_{||}^{e,i} \approx A_{||}^{e,i}T_{e,i}^{2.5}$, with $A_{||}^e \approx 10^{18}\,\mathrm{m^{-1}\,s^{-1}\,eV^{-2.5}}$ and $A_{||}^i \approx 3.3\times10^{16}\,\mathrm{m^{-1}\,s^{-1}\,eV^{-2.5}}$, one obtains for the temperatures

$$\frac{T_{e,i}^{2.5}dT_{e,i}}{1 - T_{e,i}/T_{e,i}^c} = \frac{q_{||L}^{e,i}dl^2}{2LA_{||}^{e,i}}.$$

Here $T_{e,i}^c = q_{||L}^{e,i}/(2.5\Gamma_{||L})$ are the maximum temperature values, corresponding to the whole heat flux transported with convection by the plasma particle flow only. The latter equation can be analytically integrated, providing a transcendental algebraic equation for $T_{e,i}(x,l)$, see Ref. 18. Here, however, we prefer to represent the result of integration as a polynomial algebraic equation for $\theta = T_{e,i}(l,x)/T_{e,i}(0,x)$, in the following form convenient for a fast finding of the root in question with the Newton method:

$$\theta^{3.5}\left(1 + \sum_{k=1}^{\infty}\frac{\xi_0^k\theta^k}{1+k/3.5}\right) = 1 - \left(1-\theta_L^{3.5}\right)(l/L)^2 + \sum_{k=1}^{\infty}\xi_0^k\frac{1-\left(1-\theta_L^{3.5+k}\right)(l/L)^2}{1+k/3.5}.$$

The parameters $\theta_L = T_{e,i}(L,x)/T_{e,i}(0,x)$ and $\xi_0 = T_{e,i}(0,x)/T_{e,i}^c(x)$ are external for the problem under consideration; these can be defined by including the X-point and divertor regions into the analysis. However, for the conditions of either strong recycling or detachment, expected in the DEMO divertor, heat will be transported in the SOL mostly by the heat conduction. Thus ξ_0, $\theta_L \ll 1$ and the summations in the equation above converge fast. Figure 2(a) shows the average value of θ along the main SOL, $\langle\theta\rangle$, versus the parameters θ_L and ξ_0; it is in a very narrow range of $0.86 - 0.87$. For the relation between the heat loss density and the temperatures of the plasma components average along the main SOL, $\langle T_{e,i}\rangle(x) = T_{e,i}(0,x)\langle\theta\rangle$, we get

$$q_{||L}^{e,i} = \chi A_{||}^{e,i}\langle T_{e,i}\rangle^{3.5}/L, \tag{24}$$

with

$$\chi = \frac{1 - \theta_L^{3.5} + \sum_{k=1}^{\infty}\xi_0^k\left(1-\theta_L^{3.5+k}\right)/(1+k/3.5)}{1.75\langle\theta\rangle^{3.5}}.$$

The dependence χ on the parameters θ_L and ξ_0 is displayed in Figure 2(b); roughly $\chi \approx 1 + 2.5\xi_0^2$ for small ξ_0.

In concluding this section, we assess the relation of the plasma particle loss density $\Gamma_{||L}$ to the plasma parameters averaged over the main SOL. To maintain a steady state, the outflow from the SOL into the divertor has to be exhausted, by pumping out a part $\omega_{pump} \ll 1$ of neutrals born by plasma recombination at the target plates, i.e., $\Gamma_{||L} = \omega_{pump}\Gamma_{||p}$, with the plasma flux to the plate[6]

$$\Gamma_{||p} = n_p M_p\sqrt{2T_p/m},$$

where n_p and $M_p \ge 1$ are the plasma density and Mach number, correspondingly, at the target; due to high frequency of coulomb collisions, electrons and ions have here roughly the same temperature T_p. In the main SOL, the parallel plasma momentum is lost with the perpendicular transport and friction by charge-exchange collisions with recycling neutrals. All together, these losses are characterized by the time $\tau_{loss} \sim 10^{-4}$ s and the motion equation is as follows:

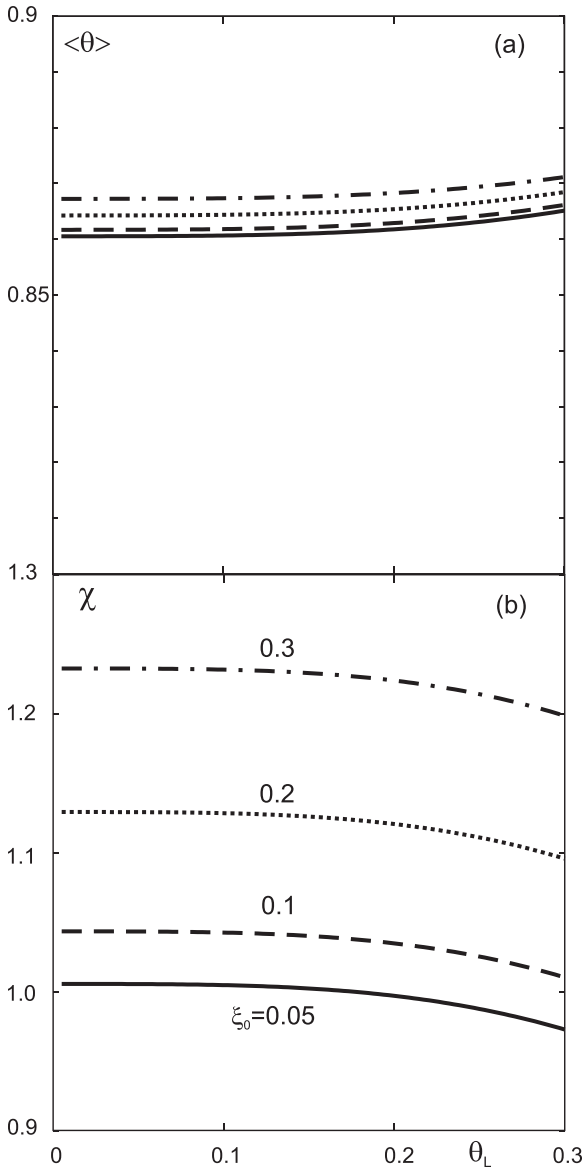

FIG. 2. The SOL averaged value $\langle\theta\rangle$ of dimensionless temperature (a) and the factor χ in the relation (23) (b) versus θ_L calculated for different magnitudes of the convection fraction: $\xi_0 = 0.05$ (solid line), 0.1 (dashed line), 0.2 (dotted line), and 0.3 (dashed-dotted line).

$$\partial_l P = -\frac{m\Gamma_{||}}{\tau_{loss}}, \tag{25}$$

with $P = n(T_e + T_i) + m\Gamma_{||}^2/n$ being the total plasma pressure. By integrating Equation (25) along the main SOL, $0 \le l \le L$, with relations (23) taken into account, one gets

$$P(0) - \Gamma_{||L}\frac{mL}{2\tau_{loss}} = P(L), \tag{26}$$

where $P(0) = n(0)[T_e(0) + T_i(0)]$ and $P(L)$ are the total pressure values at the SOL symmetry plane and at the entrance of the divertor region, respectively. P is normally reduced further in the divertor by a factor $\delta_d < 1$, the so-called "detachment degree," and at the target it approaches the level

$$P_p \equiv 2T_p n_p + m\Gamma_{||p}^2/n_p = \Gamma_{||L}\sqrt{2T_p m}\frac{M_p + 1/M_p}{\omega_{pump}}. \tag{27}$$

By introducing $\eta = n/n(0)$ and combining Equations (26) and (27), we get

$$\Gamma_{||L} = \frac{\mu}{\langle\eta\rangle\langle\theta\rangle}\frac{\langle n\rangle\langle c_s^2\rangle}{V_d}, \tag{28}$$

with $\langle c_s^2\rangle = [\langle T_e\rangle + \langle T_i\rangle]/m$, $\mu = [1 + L/(2V_d\tau_{loss})]^{-1}$ and the "divertor impact factor"

$$V_d = \sqrt{\frac{2T_p}{m}}\frac{M_p + 1/M_p}{\delta_d\omega_{pump}}.$$

To make a guess about the latter, we apply the parameters foreseen for ITER,[3] $T_p \approx 3\,\text{eV}$, $M_p = 1$, $\delta_d = 1/2$, and $\omega_{pump} \approx 10^{-2}$. This results in $V_d \approx 1.5 \times 10^6\,\text{ms}^{-1}$, exceeding significantly the ion sound velocity of $10^5\,\text{ms}^{-1}$ for $T_{e,i} \approx 200\,\text{eV}$ typical of the DEMO SOL, see Figure 3. Since $\mu, \langle\eta\rangle\langle\theta\rangle \sim 1$, the flow in the main SOL part is deeply subsonic, as it was assumed and employed above, by the assessment of the parallel heat transport. Thus, $\chi = 1$ can be used in the relation (24) for $q_{||L}^{e,i}$.

To assess $\langle\eta\rangle$ explicitly, we integrate Equation (25) from 0 to l and obtain

$$n(0)[T_e(0) + T_i(0)] = n(l)[T_e(l) + T_i(l)] + m\Gamma_{||L}\left[\frac{\Gamma_{||L}}{n(l)} + \frac{L}{2\tau_{loss}}\right]\left(\frac{l}{L}\right)^2,$$

or a quadratic equation for $\eta(l)$,

$$\eta^2(l) - \eta(l)\frac{1 - (1-\mu)(l/L)^2}{\theta(l)} + \frac{\mu^2\langle c_s^2\rangle(l/L)^2}{\theta(l)\langle\theta\rangle V_d^2} = 0,$$

with the solution of interest:

$$\eta(l) = \frac{1 - (1-\mu)(l/L)^2}{2\theta(l)} \times \left[1 + \sqrt{1 - \frac{4\mu^2\langle c_s^2\rangle\theta(l)(l/L)^2}{V_d^2\langle\theta\rangle\left[1 - (1-\mu)(l/L)^2\right]^2}}\right].$$

Since $\langle c_s^2\rangle \ll V_d^2$, a Taylor's expansion of the square root term can be done and, finally, we get

$$\langle\eta\rangle \approx \left\langle\frac{1}{\theta}\right\rangle - (1-\mu)\left\langle\frac{l^2}{L^2\theta}\right\rangle - \mu^2\frac{8 - 3\mu}{15\langle\theta\rangle}\frac{\langle c_s^2\rangle}{V_d^2}. \tag{29}$$

We have to admit that the divertor impact factor V_d is probably the most obscure among those involved in Equations (28) and (29). Therefore the influence of V_d will be examined by varying it in a broad range.

IV. RESULTS OF CALCULATIONS

Below we present the results of calculations for the "standard" set of the input parameters taken from the European DEMO project:[9,10] $r_b = 2.84\,\text{m}$, $r_s = 2.93\,\text{m}$ and $r_w = 3.13\,\text{m}$; $n(0) = 1.02 \times 10^{20}\,\text{m}^{-3}$, the volume averaged

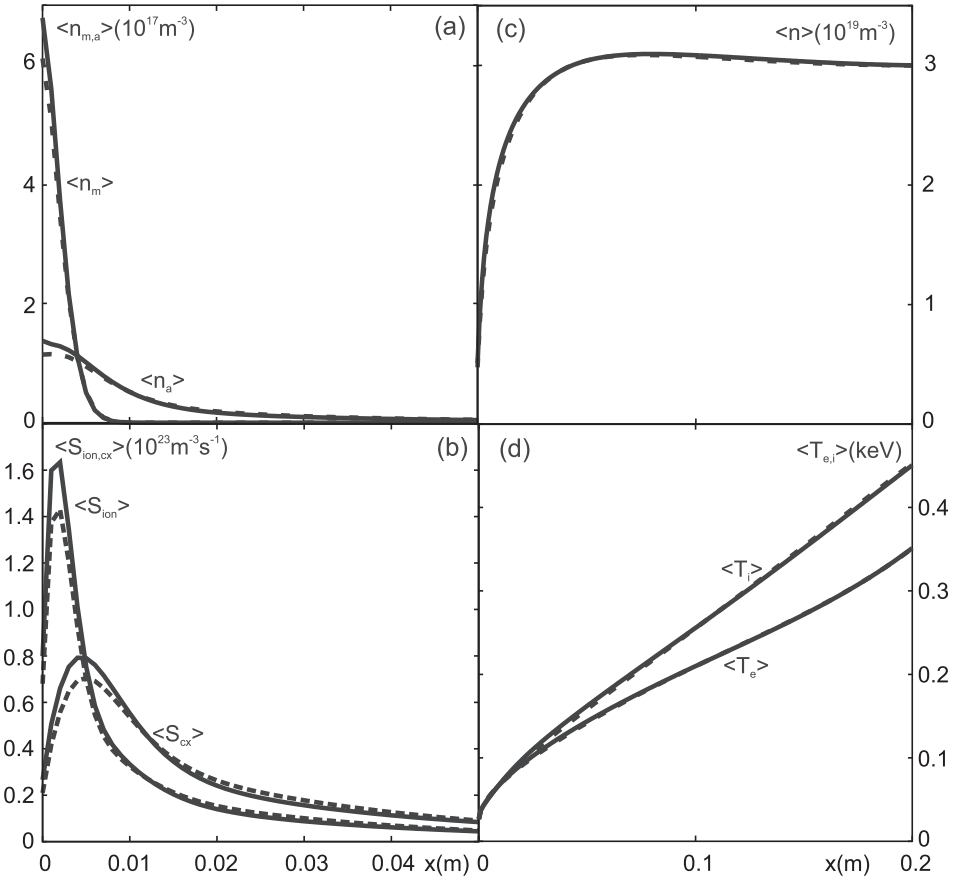

FIG. 3. The radial profiles of the SOL averaged molecule and atom densities (a), the source densities of c-x atoms and charged particles (b), plasma density (c) and electron and ion temperatures (d), calculated with the kinetic (dashed curves) and diffusion (solid curves) descriptions of c-x atoms.

density $8 \times 10^{19}\,\mathrm{m}^{-3}$ and $n(r_s) = 3 \times 10^{19}\,\mathrm{m}^{-3}$; $T_e(0) = 27.4\,\mathrm{keV}$, $T_e(r_b) = 8\,\mathrm{keV}$ and $T_i = 1.5T_e$ is assumed in the plasma core, $0 \le r \le r_b$; the heat flux densities at the separatrix $q_\perp^{e,i}(r_s) = 54\,\mathrm{kW\,m}^{-2}$; the connection length in the SOL $L_\parallel = 90\,\mathrm{m}$, the divertor impact factor $V_d = 1.5 \times 10^6\,\mathrm{ms}^{-1}$ and the e-folding lengths of the plasma parameters at the wall of tungsten, $\delta_{n,e,i} = 10^{-3}\,\mathrm{m}$. In the SOL, we assume a diffusive perpendicular plasma particle transport, $\Gamma_\perp = -D_\perp \partial_x n$, with the Bohm's diffusion and heat conduction

$$D_\perp = D_B \equiv T_e/(16eB_T), \quad \kappa_\perp^{e,i} = 1.5nD_\perp,$$

at the magnetic field of 5.7 T. The rate coefficients for inelastic collisions of neutral species with electrons and ions, k_{dis}^m, $k_{ion}^{m,a}$ and $k_{cx}^{m,a}$, are taken from Ref. 11.

Figure 3 shows the radial profiles of the SOL averaged values for the particle densities of molecules, $\langle n_m \rangle$, all atom species, $\langle n_a \rangle$, and plasma, $\langle n \rangle$; the densities of sources for c-x atoms, $\langle S_{cx} \rangle$, and charged particles, $\langle S_{ion} \rangle$; the temperatures of electrons, $\langle T_e \rangle$, and ions, $\langle T_i \rangle$. The results of calculations with the kinetic and diffusion descriptions of c-x atoms are displayed by dashed and solid curves, respectively. The profiles of $\langle n_{m,a} \rangle$ and $\langle S_{cx,ion} \rangle$, calculated with two approaches, differ maximally by 15%. The difference in the plasma parameter profiles is much smaller and can be neglected in view of uncertainties, e.g., in the perpendicular transport coefficients. Indeed, by varying the parameter $\alpha_B = D_\perp/D_B$ from 0.8 to 1.2, we get a significantly larger change in the profiles, as it is demonstrated in Figure 4 for $\langle T_{e,i} \rangle(x)$. As it was mentioned above, the divertor impact factor V_d, characterizing the losses of charged particles along the magnetic field, is probably the most vulnerable input quantity for the one-dimensional Equations (20)–(24). In Figure 5, we demonstrate the profiles of the plasma component temperatures for different V_d values calculated with either kinetic or diffusion description of c-x atoms. One can see that the decrease of V_d leads to a noticeable drop of the temperatures close to the separatrix due to the enhancement of the heat loss with

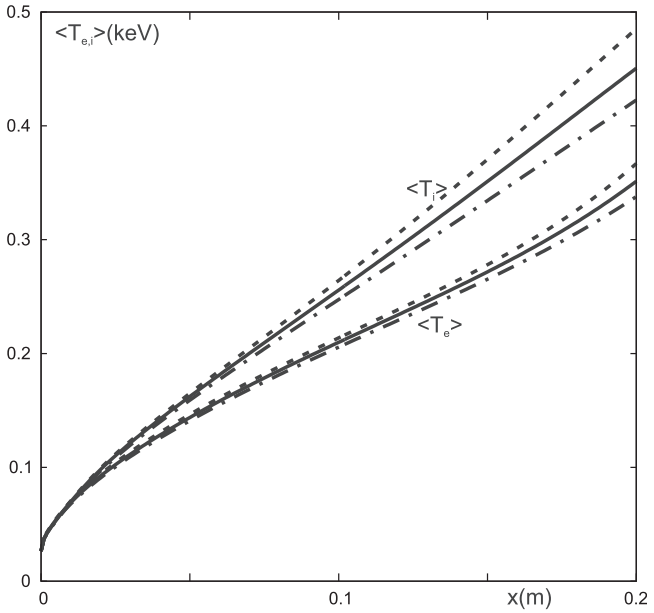

FIG. 4. The radial profiles of the SOL averaged temperatures of electrons and ions calculated with $\alpha_B = D_\perp/D_B = 1$ (solid curves), 0.8 (dashed curves), and 1.2 (dashed-dotted curves).

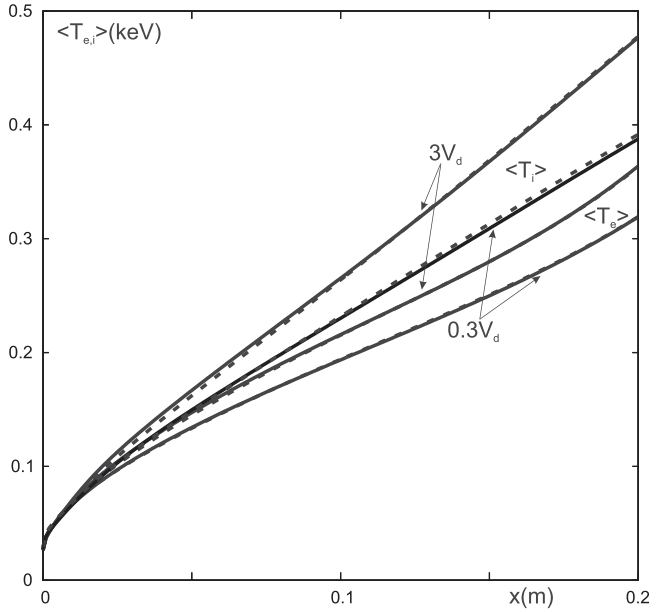

FIG. 5. The radial profiles of the SOL averaged temperatures of electrons and ions calculated for $3V_d$ and $0.3V_d$ with kinetic (dashed curves) and diffusion (solid curves) descriptions of c-x atoms.

the parallel convection of plasma particles. Although these changes are not very impressive, a firmer modeling approach has to include a coupling with a 2-D model for the X-point and divertor region, predicting reliably V_d as a function of the x-coordinate. The relatively moderate effect of the V_d value on the $\langle T_{e,i}\rangle(x)$ profiles allows to anticipate that an iterative coupling procedure can work successfully.

For the life time of the reactor wall, the energetic spectrum of c-x atoms, leaving the plasma, is of importance because such particles can have energies significantly exceeding the temperatures of the plasma components near the wall. This spectrum we characterize by the density $\gamma_{cx}(E)$ of the outflow of c-x atoms with the total energy E. It can be calculated from the distribution function $\varphi_{cx}(x, V_x, E_\perp)$ if one takes into account that $E = E_\perp + mV_x^2/2$,

$$\gamma_{cx}(E) = -\int_{-\sqrt{2E/m}}^{0} \varphi_{cx}(0, V_x, E - mV_x^2/2)V_x dV_x$$
$$= \int_0^\infty \frac{S_{cx}}{\sqrt{\pi}V_i T_i} dx \int_{-\sqrt{2E/m}}^{0} \exp\left(-\frac{E}{T_i} + \frac{U_x}{V_x}\right) dV_x$$
$$= \sqrt{\frac{E}{\pi}} \int_0^\infty \frac{S_{cx}}{T_i^{1.5}} \exp\left(-\xi - \frac{E}{T_i}\right)[1 - \xi \exp(\xi)E_1(\xi)]dx,$$

with $\xi = U_x\sqrt{m/(2E)}$. Exactly the same expression follows by calculating $\gamma_{cx}(E)$ for a given source density of c-x atoms and the Maxwellian energy distribution function for ions, an approach which can also be applied if the density of c-x atoms is calculated in the diffusion approximation.[19] The energy spectrum of the atom outflow computed with both kinetic and diffusion description of c-x atoms for three magnitudes of the divertor impact factor V_d is demonstrated in Figure 6. One can see that the diffusion approximation systematically overestimates $\gamma_{cx}(E)$ in the vicinity of its maximum but underestimates for higher energies. The latter is

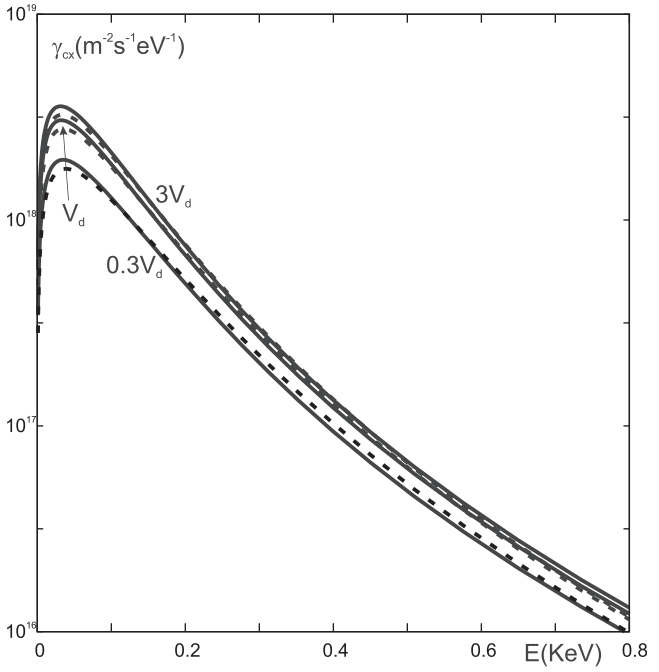

FIG. 6. Energy spectra of the outflow of c-x atoms to the wall for different magnitudes of the divertor impact factor, calculated with the kinetic (dashed curves) and diffusion (solid curves) descriptions of c-x atoms.

also mimicked in the heat load density on the wall due to the outflow of c-x atoms

$$q_{cx} = \int_0^\infty \gamma_{cx}(E)EdE.$$

In Figure 7 q_{cx} is displayed as a function of V_d calculated for different magnitudes of the parameter $\alpha_B = D_\perp/D_B$, with

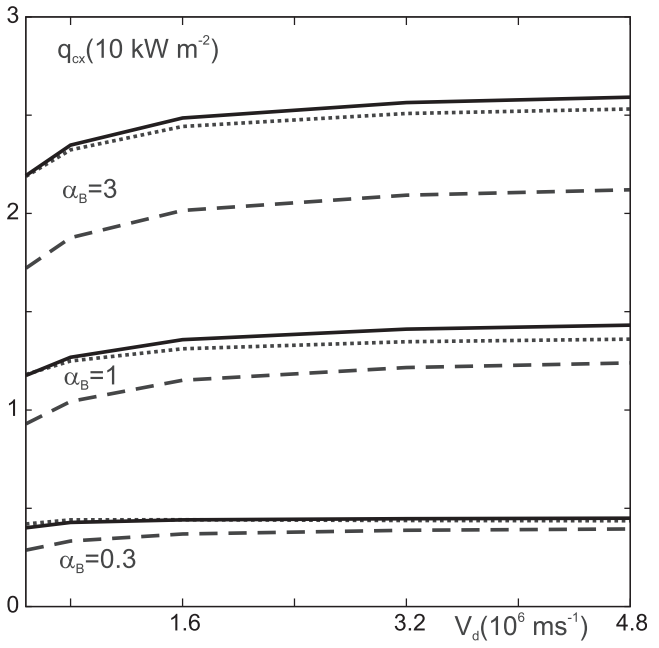

FIG. 7. The density of the heat flux transported to the wall by atoms versus the divertor impact factor V_d and for different magnitudes of the parameter $\alpha_B = D_\perp/D_B$, found with either the kinetic (dotted curves) or diffusion (dashed curves) description of c-x atoms, and by doing in the latter case, the last calculation for c-x atoms kinetically (solid curves).

either kinetic or diffusion description of c-x neutrals. The underestimation in the diffusion approximation of $\gamma_{cx}(E)$ for large E results in q_{cx} smaller by maximally $20\% - 30\%$. This error can be significantly reduced if after the convergence of coupled plasma-neutral calculations, the final computation of c-x atoms is done kinetically. The dependencies of q_{cx} on V_d and α_B found in this case are also shown in Figure 7.

V. CONCLUSIONS

The main aim of the present study is to validate the diffusion approximation to describe atoms generated by the charge-exchange of neutral species recycling from the wall of a fusion reactor. The demand to apply such an approximation is dictated by the high level of accident errors, "noise," in the characteristics of neutral species computed by the statistical Monte Carlo methods, leading to a slow convergence of coupled neutral-plasma computations. The present consideration is confined to the main SOL, and equations for the variation of the parameters with the distance from the wall are integrated. It is demonstrated that the solving of the kinetic equation for c-x atoms, represented in the integral form, can be accelerated at least by a factor of 30 if the arising integrals over the velocity space are evaluated by an approximate pass method. A possibility to apply this approach to 2-D or 3-D situations has not been proven yet. Therefore, the credibility of the diffusion approximation, being strictly valid for low temperatures when the ionization rate coefficient k^a_{ion} is much smaller than that of the charge-exchange, k^a_{cx}, has been thoroughly investigated for the SOL conditions where $k^a_{ion} \sim k^a_{cx}$. By applying this approximation, which can be easily generalized for 2D and 3D configurations, calculations for c-x atoms can be speeded up additionally by a factor of 10^3. To perform a self-consistent modeling of the plasma in the SOL, equations for the variation across the flux surfaces of the density and temperatures of electrons and ions, averaged along the SOL, are deduced by integrating the two-dimensional fluid equations along the magnetic field. It is demonstrated that the parallel outflows of heat from the integration domain towards the divertor can be firmly assessed and related to the parameters averaged along the main SOL only. In the case of plasma particle losses, the so-called "divertor impact factor" has to be introduced into the model additionally.

Coupled 1D models for neutral and charged species, either with kinetic or with diffusion description of c-x atoms, have been numerically realized and calculations performed for the input parameters from the European DEMO project. It is shown that the diffusion approximation works extremely good, by providing practically the same profiles across flux surfaces for the SOL averaged plasma parameters as those obtained with the kinetic description for c-x atoms. The maximum discrepancy between the two approaches appears for the characteristics of c-x species themselves. So their energy flux onto the wall is underestimated with the diffusion approximation by 20%–30%. Nonetheless, this discrepancy can be significantly reduced if the plasma parameters found in the latter case are used for the final kinetic calculation of c-x atoms. Our investigation permits to validate firmly the diffusion approximation for c-x atoms for the SOL conditions of relatively high temperatures with comparable rates of ionization and charge-exchange and allows an enormous saving of the CPU time by several orders of magnitude. To our mind, this conclusion can also be practical for 2-D and 3-D geometries; however, careful peculiar considerations have to be performed also in these situations.

In the present study, an idealized situation with a clearance between the wall and separatrix constant along the SOL has been assumed. In a realistic case, this changes along the flux surfaces due to shift, elongation, and triangularity of the surfaces. Nonetheless, we want to stress that the one-dimensional models for neutral and plasma parameters in the main SOL are also relevant to these conditions. The penetration depths for neutral species are normally much shorter than the characteristic distance where the magnetic geometry changes in the poloidal direction. Thus, a one-dimensional description of neutrals, recycling from the wall, can be applied individually at different poloidal positions, see Ref. 20. In Equations (20)–(22) for charged particles, the terms $S^{m,a}_{ion}$ and S_{cx}, arising due to the presence of neutrals, are linearly related to their densities. If the latter are calculated in the one-dimensional approximation for poloidal positions with noticeably different distances between the flux surfaces, one can straightforwardly perform averaging in the equations for the plasma parameters, if these change weakly along the main SOL.

APPENDIX: VELOCITY DISTRIBUTION OF c-x ATOM SOURCE

In the kinetic Boltzmann equation for c-x atoms,[7] the source term due to collisions with ions is as follows:

$$C_{cx} = \varphi_i(\mathbf{v})[n_m k^m_{cx} + \int \varphi_a(\mathbf{v}')k^a_{cx}(E)d^3\mathbf{v}'],$$

where $\mathbf{v}$ and $\mathbf{v}'$ are the velocities, φ_i and φ_a, the velocity distribution functions of ions and atoms, respectively. In a very broad range of the energy $E = m|\mathbf{v} - \mathbf{v}'|^2/4$ of ion-atom relative motion, $1\,\mathrm{eV} \lesssim E \lesssim 10\,\mathrm{keV}$, the rate coefficient of atom charge-exchange collisions changes very weakly, $k^a_{cx}(E) \sim E^{0.3}$. Thus, without a large error, one can use for this the values, computed for the characteristic energies of interacting ions and atoms, $E_i = 1.5T_i$ and E_a, correspondingly, with the latter being equal to E^i_{bs} and E^{cx}_{bs} for backscattered species, E_{fc} and $E_{cx} = W_{cx}/n_{cx}$ for f-c and c-x atoms where W_{cx} is the thermal capacity of c-x atoms defined after Equation (19). With an accuracy of 2%,

$$k^a_{cx} \approx 10^{-14}\left(\frac{E_i + E_a}{A_i}\right)^{0.3},$$

where k^a_{cx} is measured in $\mathrm{m^3\,s^{-1}}$, E_i, E_a—in eV and A_i is the atomic weight of the hydrogen isotope in question.

With this approximation, we get

$$C_{cx} \approx (n_m k^m_{cx} + n^i_{bs}k^{bs-i}_{cx} + n^{cx}_{bs}k^{bs-cx}_{cx} + n_{fc}k^{fc}_{cx} + n_{cx}k^{cx}_{cx})\varphi_i(\mathbf{v}).$$

The cross-section of charge-exchange is much larger than that of the elastic collisions between hydrogen ions and atoms. Therefore, the ion velocity distribution function is practically unperturbed by the charge transfer. By choosing $\varphi_i(\mathbf{v})$, we take into account that (i) the ion thermalization time in the DEMO SOL will be of 0.1 ms, i.e., much shorter than the characteristic transport times along and across the SOL of 10 ms, see Section III B; (ii) ions are magnetized so their mass velocity in the x-direction across the magnetic field is much smaller than V_{th}. Thus the Maxwellian distribution function can be assumed for ions

$$\varphi_i\left(V_x, V_\perp = \sqrt{\frac{2E_\perp}{m}}\right) = \frac{n}{\sqrt{\pi}V_{th}T_i}\exp\left(-\frac{V_x^2}{V_{th}^2} + \frac{E_\perp}{T_i}\right).$$

By integrating C_{cx} over $E_\perp$, one gets the source term assumed in Equation (5), $S_{cx}\frac{\exp\left(-V_x^2/V_{th}^2\right)}{\sqrt{\pi}V_{th}}$.

[1]J. Li, *Fusion Physics* (International Atomic Energy Agency, Vienna, 2012).
[2]D. P. Landau and K. Binder, *A Guide to Monte Carlo Simulations in Statistical Physics* (University Printing House, Cambridge, 2015).
[3]A. Loarte, B. Lipschultz, A. S. Kukushkin, G. F. Matthews, P. C. Stangeby, N. Asakura, G. F. Counsell, G. Federici, A. Kallenbach, K. Krieger *et al.*, "Power and particle control," Nucl. Fusion **47**(6), S203–S263 (2007); A. S. Kukushkin, H. D. Pacher, G. W. Pacher, G. Janeschitz, D. Coster, A. Loarte, and D. Reiter, "Scaling laws for edge plasma parameters in ITER from two-dimensional edge modeling," *ibid.* **43**(8), 716–723 (2003).
[4]N. Horsten, W. Dekeyser, G. Samaey, and M. Baelmans, "Comparison of fluid neutral models for one-dimensional plasma edge modeling with a finite volume solution of the Boltzmann equation," Phys. Plasmas **23**(1), 012510 (2006).
[5]D. Reiter, M. Baelmans, and P. Borner, "The EIRENE and B2-EIRENE codes," Fusion Sci. Technol. **47**(2), 172–186 (2005).
[6]P. C. Stangeby, *The Plasma Boundary of Magnetic Fusion Devices* (Institute of Physics Publishing, Bristol and Philadelphia, 2000).
[7]S. Rehker and H. Wobig, "A kinetic model for the neutral gas between plasma and wall," Plasma Phys. **15**(11), 1083–1097 (1973).
[8]J. Mathews and R. L. Walker, *Mathematical Methods of Physics*, 2nd ed. (Benjamin, Menlo Park, 1970).
[9]G. Federici, R. Kemp, D. Ward, C. Bachmann, T. Franke, S. Gonzalez, C. Lowry, M. Gadomska, J. Harman, B. Meszaros, C. Morlock, F. Romanelli, and R. Wenninger, "Overview of EU DEMO design and R&D activities," Fusion Eng. Des. **89**(7–8), 882–889 (2014).
[10]R. Wenninger, F. Arbeiter, J. Aubert, L. Aho-Mantila, R. Albanese, R. Ambrosino, C. Angioni, J.-F. Artaud, M. Bernert, E. Fable, A. Fasoli, G. Federici, J. Garcia, G. Giruzzi, F. Jenko, P. Maget, M. Mattei, F. Maviglia, E. Poli, G. Ramogida, C. Reux, M. Schneider, B. Sieglin, F. Villone, M. Wischmeier, and H. Zohm, "Advances in the physics basis for the European DEMO design," Nucl. Fusion **55**(6), 063003 (2015).
[11]R. K. Janev, W. D. Langer, K. J. Evans, and D. E. J. Post, *Elementary Processes in Hydrogen-Helium Plasmas* (Springer, Hamburg, 1987).
[12]M. J. Maron and R. J. Lopez, *Numerical Analysis: A Practical Approach* (International Thomson Publishing, New York, 1991).
[13]V. Kotov, private communication (2016).
[14]B. Lehnert, "Screening of a high-density plasma from neutral gas penetration," Nucl. Fusion **8**(3), 173–181 (1968).
[15]M. Z. Tokar, "The possible nature of the localized recycling effect on TGHE plasma edge in tokamaks," Plasma Phys. Controlled Fusion **35**(9), 1119–1135 (1993).
[16]L. W. Kantorowitsch and W. I. Krylow, *Approximate Methods of Higher Analysis* (Interscience Publishers Inc., New York, 1958).
[17]L. Spitzer and R. Härm, "Transport phenomena in a completely ionized gas," Phys. Rev. **89**(5), 977 (1953).
[18]M. Z. Tokar, M. Kobayashi, and Y. Feng, "Improved two-point model for limiter scrape-off layer," Phys. Plasmas **11**(10), 4610–4615 (2004).
[19]M. Z. Tokar, M. Beckers, and W. Biel, "Erosion of installations in ports of a fusion reactor by hot fuel atoms," J. Nucl. Mater (in press).
[20]M. Z. Tokar, "Effect of magnetic geometry on transport of neutral particles locally entering confined plasma volume," Phys. Plasmas **16**(9), 094506 (2009).